ISSN 2176-5480

22nd International Congress of Mechanical Engineering (COBEM 2013)
November 3-7, 2013, Ribeirão Preto, SP, Brazil

HYBRID SOLUTION FOR SIMULTANEOUSLY DEVELOPING NEWTONIAN FLOW IN CIRCULAR TUBES: EFFECT OF THE VISCOUS DISSIPATION ON THE TEMPERATURE FIELD

Diana Patrícia Santos de Souza
Emanuel Negrão Macêdo
João Nazareno Nonato Quaresma
School of Chemical Engineering, ITEC, Universidade Federal do Pará, UFPA, Campus Universitário do Guamá, Rua Augusto Corrêa, 01, 66075-110, Belém, PA, Brazil.
dianapssouza@hotmail.com
enegrao@ufpa.br
quaresma@ufpa.br

Abstract: *The Generalized Integral Transform Technique (GITT) is applied to the problem of simultaneously developing flow of a Newtonian fluid in a circular tube. The effect of viscous dissipation is also considers to evaluate its influence in the temperature field. A streamfunction formulation is adopted in order to avoid the singularity of the auxiliary eigenvalue problem in terms of Bessel functions at the centerline of the duct when the GITT approach is applied. Results for the velocity and temperature fields, as well as quantities of practical interest such as Nusselt numbers are computed for different Brinkman and Prandtl numbers, which are tabulated and graphically presented as functions of the dimensionless coordinates. Critical comparisons with previous results in the literature are also performed, in order to validate the numerical codes developed in the present work and to demonstrate the consistency of the final results.*

Keywords: *Generalized integral transform technique, Newtonian fluids, Brinkman numbers, simultaneously developing laminar flow, streamfunction formulation.*

1. INTRODUCTION

The effect of viscous dissipation may become very important in various flow settings occurring in engineering practice, for example, in micro channel flows considered for the design of Micro Electro Mechanical Systems (MEMS). The viscous dissipation highly affects heat transfer processes whenever the fluid used has a low thermal conductivity and a high viscosity, as well as for fluid flow in small cross section ducts, and a small wall heat flux. In addition, the effect of viscous heating increases greatly with an increase in the mass flow rate; consequently, this effect becomes more important under forced convection heat transfer. To examine the thermal entrance regime in various duct geometries, prediction of the effect of viscous dissipation is a key point. One of the most important consequences of the effect of viscous dissipation is in the evaluation of the local Nusselt number that can theoretically be obtained by suitable mathematical modeling and subsequent solution of the problem addressed (Dehkordi, 2009; Dehkordi, 2010). The advancement of solution techniques has allowed the opening of new directions in search of fluid flow in ducts, considering that are modeled by complicated equations, and often nonlinear, which have analytical solutions only in specific cases. When it comes to obtain reliable results, the use of a solution technique that leads to accurate results for such flows is essential.

Along the years, the literature reveals the progressive development of hybrid schemes based on eigenfunction expansions, which recently, due to the development of symbolic computation platforms, have became more attractive due to the reduction on the analytical development effort (Cotta, 1990; Cotta, 1998; Santos *et al*., 2001; Cotta and Mikhailov, 2006). In this class, the Integral Transform Method (Cotta, 1993) was gradually expanded in its applicability, under the label of the Generalized Integral Transform Technique (GITT), and extensively employed in heat/mass transfer and fluid flow problems (Silva and Cotta, 1992; Perez-Guerrero and Cotta, 1992; Machado and Cotta, 1995; Perez-Guerrero *et al*., 2000; Pereira *et al*., 2000), including fluid flow problems under either the boundary layer or the full Navier–Stokes formulations (Silva and Cotta, 1992; Perez-Guerrero and Cotta, 1992; Machado and Cotta, 1995; Perez-Guerrero *et al*., 2000; Pereira *et al*., 2000; Paz *et al*., 2007). In such contributions, the preference for the streamfunction-only formulation in two-dimensional situations is notorious, in light of the elimination of the pressure field and automatic satisfaction of the continuity equation. In the case of the streamfunction-only formulation, the appropriate eigenfunction expansion for the velocity problem is in general proposed based on a fourth-order eigenvalue problem related to the analytical solution of the linear biharmonic equation for vanishing Reynolds number (Pereira *et al*., 2000). Problems related to the Cartesian coordinates system were more frequently studied in comparison to those propositions of eigenfunction expansions in the cylindrical coordinates system (Pereira *et al*., 2000; Paz *et al*., 2007), possibly due to the inherent difficulties in avoiding the singularities of the fourth-order eigenvalue problem at the circular duct centerline for a full cylindrical region. These difficulties were circumvented in a recent work dealing with

ISSN 2176-5480

the boundary layer equations (Paz *et al*., 2007), by adopting an also recently introduced eigenvalue problem (Paz *et al*., 2007), which accounts for the singularities at the central radial position.

In this context, the GITT approach with its intrinsic characteristic of finding solutions with automatic global error control, opened up an alternative perspective in benchmarking and covalidation for such classical test problems. The GITT methodology was already successfully employed in the solution of the boundary-layer formulation version of this same problem, by adopting an appropriate fourth-order eigenvalue problem in the cylindrical coordinates system that could exactly deal with the singularities of the Bessel functions at the tube centerline (Paz *et al*., 2007). The present work is thus aimed at utilizing the ideas in the GITT approach to construct a hybrid analytical-numerical solution of the continuity, momentum and energy equations for a Newtonian fluid flowing in the entrance region of circular tubes taking into account the effect of viscous dissipation, and for this purpose, the boundary-layer formulation in terms of streamfunction formulation is adopted in order to avoid singularities in the auxiliary eigenvalue problem expressed as Bessel functions at the centerline of the duct. Comparisons with previous work in the literature are also made for typical situations in order to validate the numerical code developed here and to demonstrate the consistency of results produced.

2. MATHEMATICAL FORMULATION

Laminar forced convection in simultaneously developing flow of a Newtonian fluid in a circular tube is considered as show in Figure 1. The flow is assumed to be incompressible and the effect of viscous dissipation is also considered to evaluate its influence in the temperature field and physical properties are taken as constants. The steady two-dimensional continuity, Navier-Stokes and energy equations in cylindrical coordinates are used to model the flow. Within the range of validity of the boundary layer hypothesis, such equations are written in dimensionless form as:

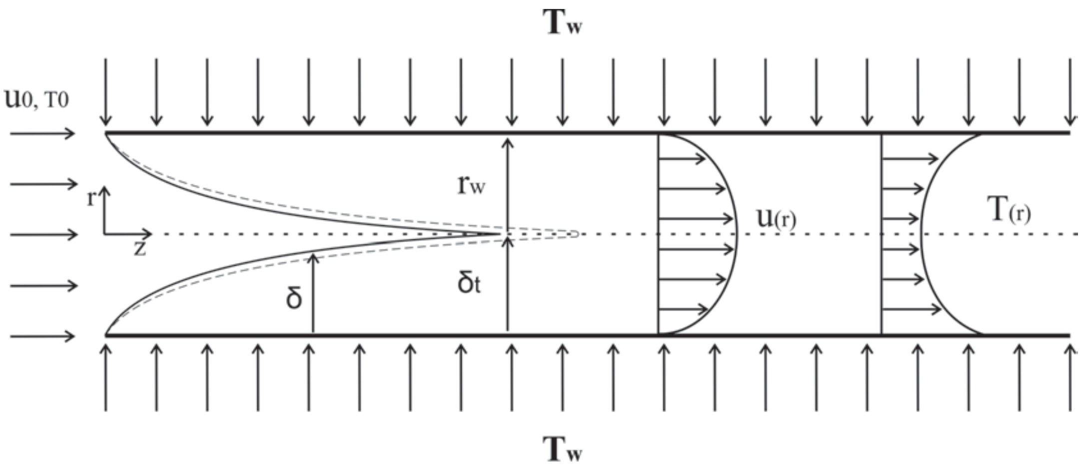

Figure 1. Geometry and coordinates system for simultaneously developing flow in circular duct.

Continuity equation:

$$\frac{1}{r}\frac{\partial(rv_r)}{\partial r}+\frac{\partial v_z}{\partial z}=0 \tag{1}$$

Momentum equations:

$$v_r\frac{\partial v_z}{\partial r}+v_z\frac{\partial v_z}{\partial z}=-\frac{\partial p}{\partial z}+\frac{2}{\mathrm{Re}}\frac{1}{r}\frac{\partial}{\partial r}\left(r\frac{\partial v_z}{\partial r}\right) \tag{2}$$

$$-\frac{\partial p}{\partial r}=0 \tag{3}$$

Energy equation:

$$v_r\frac{\partial T}{\partial r}+v_z\frac{\partial T}{\partial z}=\frac{2}{Pe}\frac{1}{r}\frac{\partial}{\partial r}\left(r\frac{\partial T}{\partial r}\right)+2\frac{Br}{Pe}\left(\frac{\partial v_z}{\partial r}\right)^2 \tag{4}$$

Equations (1)-(4) are subjected to following boundary conditions:

$$v_z(r,0)=1 \;\; ; \;\; T(r,0)=1 \tag{5,6}$$

$$v_r(0,z)=0 \;\; ; \;\; \frac{\partial v_z(0,z)}{\partial r}=0 \; ; \;\; \frac{\partial T(0,z)}{\partial r}=0 \tag{7-9}$$

$$v_z(1,z)=0 \;\; ; \;\; v_r(1,z)=0 \;\; ; \;\; T(1,z)=0 \tag{10-12}$$

The dimensionless groups in the above equations are defined as:

$$r=\frac{r^*}{r_w} \;\; ; \;\; z=\frac{z^*}{r_w} \;\; ; \;\; v_r=\frac{v_r{}^0}{u_0} \;\; ; \;\; v_z=\frac{v_z{}^0}{u_0} \;\; ; \;\; T=\frac{T^*-T_w}{T_0-T_w} \;\; ; \;\; p=\frac{p^*}{\rho u_0{}^2} \tag{13}$$

$$\mathrm{Re}=\frac{2\rho u_0 r_w^*}{m} \; ; \;\; \mathrm{Pr}=\frac{m}{\rho\alpha} \;\; ; \;\; Pe=\mathrm{Re}\,\mathrm{Pr}=\frac{2u_0 r_w}{\alpha} \;\; ; \;\; Br=\frac{m u_0^2}{(T_0-T_w)k}$$

Now, Eqs. (1)-(13) equations are expressed in terms of the streamfunction-only formulation in order to automatically satisfy the continuity equation and eliminate the pressure field, in the form:

$$\frac{1}{r}\frac{\partial\psi}{\partial z}\left(\frac{1}{r}\frac{\partial^3\psi}{\partial r^3}-\frac{3}{r^2}\frac{\partial^2\psi}{\partial r^2}+\frac{3}{r^3}\frac{\partial\psi}{\partial r}\right)-\frac{1}{r}\frac{\partial\psi}{\partial r}\left(\frac{1}{r}\frac{\partial^3\psi}{\partial r^2\partial z}-\frac{1}{r^2}\frac{\partial^2\psi}{\partial r\partial z}\right)=\frac{2}{\mathrm{Re}}\frac{\partial}{\partial r}\left\{\frac{1}{r}\frac{\partial}{\partial r}\left[r\left(\frac{1}{r}\frac{\partial^2\psi}{\partial r^2}-\frac{1}{r^2}\frac{\partial\psi}{\partial r}\right)\right]\right\} \tag{14}$$

$$\frac{1}{r}\frac{\partial\psi}{\partial z}\frac{\partial T}{\partial r}-\frac{1}{r}\frac{\partial\psi}{\partial r}\frac{\partial T}{\partial z}=\frac{2}{Pe}\frac{1}{r}\frac{\partial}{\partial r}\left(r\frac{\partial T}{\partial r}\right)+2\frac{Br}{Pe}\left(\frac{1}{r}\frac{\partial^2\psi}{\partial r^2}-\frac{1}{r^2}\frac{\partial\psi}{\partial r}\right)^2 \tag{15}$$

The streamfunction is defined in terms of the dimensionless velocity components in the longitudinal (r) and transversal (z) directions, respectively, as

$$v_r=\frac{1}{r}\frac{\partial\psi}{\partial z}; \quad v_z=-\frac{1}{r}\frac{\partial\psi}{\partial r} \tag{16,17}$$

The boundary conditions expressed in terms of the streamfunction are given by:

$$\frac{\psi(r,0)}{r}=C_1-\frac{r}{2} \;\; ; \;\; T(r,0)=1 \tag{18,19}$$

$$\lim_{r\to 0}\frac{\psi(r,0)}{r}=C_1 \;\; ; \;\; \lim_{r\to 0}\frac{\partial}{\partial r}\left[\frac{1}{r}\frac{\partial\psi(r,z)}{\partial r}\right]=0 \;\; ; \;\; \frac{\partial T(0,z)}{\partial r}=0 \tag{20-22}$$

$$\frac{\partial\psi(1,z)}{\partial r}=0 \;\; ; \;\; \psi(1,z)=C_2 \;\; ; \;\; T(1,z)=0 \tag{23-25}$$

where C_1 and C_2 are constants that specify the streamfunction values at the channel centerline and wall. The constant q warrants the global mass conservation. Such constants as relates by using the boundary conditions, to yield

$$C_2=C_1-\frac{q}{2} \tag{26}$$

One may arbitrarily specify C_1=0, so that C_2= -1/2 and q=1.

ISSN 2176-5480

To improve the computational performance is convenient define a filter that reproduces the fully developed flow solution in order to homogenize the boundary conditions. Therefore, the simple filter adopted is written as

$$\psi(r,z)=\psi_\infty(r)+\phi(r,z);\quad \psi_\infty(r)=r^2\left(\frac{r^2}{2}-1\right)\tag{27,28}$$

This is a commonly used strategy in the integral transform approach that is equivalent to the separation of the steady state solution in a transient problem, which acts by filtering the equation source terms responsible for the slower convergence rates in non-homogeneous problems. Then, after the substitution of Eq. (27), the problem formulation is rewritten as:

$$\begin{aligned}&\frac{1}{r}\frac{\partial\phi}{\partial z}\left(\frac{\partial^3\phi}{\partial r^3}-\frac{3}{r}\frac{\partial^2\phi}{\partial r^2}+\frac{3}{r^2}\frac{\partial\phi}{\partial r}+\frac{d^3\psi_\infty}{dr^3}-\frac{3}{r}\frac{d^2\psi_\infty}{dr^2}+\frac{3}{r^2}\frac{d\psi_\infty}{dr}\right)-\frac{\partial^3\phi}{\partial r^2\partial z}\left(\frac{1}{r}\frac{\partial\phi}{\partial r}+\frac{1}{r}\frac{d\psi_\infty}{dr}\right)+\frac{1}{r}\frac{\partial^2\phi}{\partial r\partial z}\left(\frac{1}{r}\frac{\partial\phi}{\partial r}+\frac{1}{r}\frac{d\psi_\infty}{dr}\right)=\\&\frac{2}{\mathrm{Re}}\left(\frac{\partial^4\phi}{\partial r^4}-\frac{2}{r}\frac{\partial^3\phi}{\partial r^3}+\frac{3}{r^2}\frac{\partial^2\phi}{\partial r^2}-\frac{3}{r^3}\frac{\partial\phi}{\partial r}+\frac{d^4\psi_\infty}{dr^4}-\frac{2}{r}\frac{d^3\psi_\infty}{dr^3}+\frac{3}{r^2}\frac{d^2\psi_\infty}{dr^2}-\frac{3}{r^3}\frac{d\psi_\infty}{dr}\right)\end{aligned}\tag{29}$$

$$\frac{1}{r}\frac{\partial\phi}{\partial z}\frac{\partial T}{\partial r}-\frac{1}{r}\frac{\partial\phi}{\partial r}\frac{\partial T}{\partial z}-\frac{1}{r}\frac{d\psi_\infty}{dr}\frac{\partial T}{\partial z}=\frac{2}{Pe}\frac{1}{r}\frac{\partial}{\partial r}\left(r\frac{\partial T}{\partial r}\right)+2\frac{Br}{Pe}\left(\frac{1}{r}\frac{\partial^2\phi}{\partial r^2}-\frac{1}{r^2}\frac{\partial\phi}{\partial r}+\frac{1}{r}\frac{d^2\psi_\infty}{dr^2}-\frac{1}{r^2}\frac{d\psi_\infty}{dr}\right)^2\tag{30}$$

$$\frac{\phi(r,0)}{r}=C_1-\frac{r}{2}-\frac{\psi_\infty(r)}{r};\quad T(r,0)=1\tag{31,32}$$

$$\lim_{r\to0}\frac{\phi(r,0)}{r}=0;\quad \lim_{r\to0}\frac{\partial}{\partial r}\left[\frac{1}{r}\frac{\partial\phi(r,z)}{\partial r}\right]=0;\quad \frac{\partial T(0,z)}{\partial r}=0\tag{33-35}$$

$$\frac{\partial\phi(1,z)}{\partial r}=0;\quad \psi(1,z)=0;\quad T(1,z)=0\tag{36-38}$$

2.1 Solution methodology

In applying the GITT approach in the solution of the PDE system given by Eqs. (29) to (38), due to the homogeneous characteristics of the boundary conditions in the r direction, it is more appropriate to choose this direction for the process of integral transformation. Therefore, the auxiliary eigenvalue problems related to the velocity and temperature fields are taken as follows:

- For the velocity field:

$$E^4\mathrm{X}_i(r)=-\lambda_i E^2\mathrm{X}_i(r)\tag{39}$$

$$\lim_{r\to0}\left[\frac{\mathrm{X}_i(r)}{r}\right]=0;\quad \lim_{r\to0}\left\{\frac{d}{dr}\left[\frac{1}{r}\frac{d\mathrm{X}_i(r)}{dr}\right]\right\}=0\tag{40,41}$$

$$\mathrm{X}_i(1)=0;\quad \frac{d\mathrm{X}_i(1)}{dr}=0\tag{42,43}$$

where,

$$E^2=r\frac{d}{dr}\left(\frac{1}{r}\frac{d}{dr}\right)=\frac{d^2}{dr^2}-\frac{1}{r}\frac{d}{dr}\quad;\quad E^4=E^2E^2=\frac{d^4}{dr^4}-\frac{2}{r}\frac{d^3}{dr^3}+\frac{3}{r^2}\frac{d^2}{dr^2}-\frac{3}{r^3}\frac{d}{dr}\tag{44,45}$$

The eigenfunction and the transcendental expression to calculate the eigenvalues are given, respectively, by

$$\mathrm{X}_i(r)=r^2-\frac{rJ_1(\lambda_i r)}{J_1(\lambda_i)}\quad;\quad J_2(\lambda_i)=0\ ,\ i=1,2,3,...\tag{46,47}$$

The eigenfunctions of this eigenvalue problem enjoy the following orthogonality property

$$\int_0^1\frac{\mathrm{X}_i'(r)\mathrm{X}_j'(r)}{r}dr=-\int_0^1\frac{\mathrm{X}_iE^2\mathrm{X}_j'}{r}dr=\begin{cases}0\ ,\ i\neq j\\ M_i\ ,\ i=j\end{cases}\tag{48}$$

ISSN 2176-5480

The normalization integral M_i is then computed from

$$M_i = \int_0^1 \frac{1}{r}\left(X_i^{'}(r)\right)^2 dr = \frac{\lambda_i^2}{2} \tag{49}$$

- For temperature field:

$$\frac{d}{dr}\left(r\frac{d\Gamma_i(r)}{dr}\right) + \mu_i^2 r\Gamma_i(r) = 0 \tag{50}$$

$$\frac{d\Gamma_i(r)}{dr} = 0; \qquad \Gamma_i(r) = 0 \tag{51,52}$$

Similarly, problem (50) is solved analytically, to furnish the eigenfunctions, transcendental equation to compute the eigenvalues, orthogonality property and normalization integral, respectively, as

$$\Gamma_i(r) = J_0\left(\mu_i r\right); \qquad J_0\left(\mu_i\right) = 0 \ , \ i = 1,2,3,... \tag{53,54}$$

$$\int_0^1 r\Gamma_i(r)\Gamma_j(r)dr = \begin{cases} 0 \ , \ i \neq j \\ N_i \ , \ i = j \end{cases}; \qquad N_i = \int_0^1 r\Gamma_i^2(r)dr = \frac{J_1^2(\mu_i)}{2} \tag{55,56}$$

The eigenvalue problems defined by Eqs. (39) to (56) allow for the definition of the following integral transform pairs.

- For the velocity field:

$$\bar{\phi}(z) = -\frac{1}{M_i}\int_0^1 \frac{E^2 X_i(r)}{r}\phi(r,z)dr, \quad \text{Transform} \tag{57}$$

$$\phi(r,z) = \sum_{i=1}^{\infty} X_i(r)\bar{\phi}_i(z), \quad \text{Inverse} \tag{58}$$

- For the temperature field;

$$\bar{T}(z) = \frac{1}{N_i}\int_0^1 r\Gamma_i(r)T(r,z)dr, \quad \text{Transform} \tag{59}$$

$$T(r,z) = \sum_{i=1}^{\infty} \Gamma_i(r)\bar{T}_i(z), \quad \text{Inverse} \tag{60}$$

We can now accomplish the integral transformation of the original partial differential system given by Eqs. (29)-(38). For this purpose Eq. (29) is multiplied by $[X_i(r)/r]$ and integrated over the domain [0,1] in r and the inverse formula given Eq. (58) is employed, similarly, the energy equation, Eq. (30), is multiplied by $[\Gamma_i(r)/r]$ and also is integrates over the domain [0,1] in the r direction, and the inverse formula given by Eqs. (58) and (60) are employed. After the appropriate manipulations, the following coupled ordinary differential system results are utilized for the calculation of the transformed potentials:

$$\sum_{j=1}^{\infty} A_{ij}\frac{d\bar{\phi}_j}{dz} = \frac{2}{\text{Re}}B_i \qquad i = 1,2,3,... \tag{61}$$

$$\sum_{j=1}^{\infty} C_{ij}\frac{d\bar{\phi}_j}{dz} + \sum_{j=1}^{\infty} D_{ij}\frac{d\bar{T}_j}{dz} = -\frac{2}{Pe}\mu_i^2\bar{T}_i(z)N_i + \frac{2Br}{Pe}E_i \qquad i = 1,2,3,... \tag{62}$$

$$\bar{\phi}_i(0) = \bar{f}_i; \qquad \bar{T}_i(0) = \bar{g}_i \tag{63,64}$$

where,

$$A_{ij} = A1_{ij} + A2_{ij} + A3_{ij}\,; \quad A1_{ij} = \int_0^1 \frac{X_i(r)X_j(r)}{r^2}\left(\frac{\partial^3\phi}{\partial r^3} - \frac{3}{r}\frac{\partial^2\phi}{\partial r^2} + \frac{3}{r^2}\frac{\partial\phi}{\partial r} + \frac{\partial^3\psi_\infty}{\partial r^3} - \frac{3}{r}\frac{\partial^2\psi_\infty}{\partial r^2} + \frac{3}{r^2}\frac{\partial\psi_\infty}{\partial r}\right)dr \tag{65,66}$$

$$A2_{ij} = \int_0^1 \frac{X_i(r)X_j''(r)}{r}\left(\frac{1}{r}\frac{\partial\phi}{\partial r} + \frac{1}{r}\frac{\partial\psi_\infty}{\partial r}\right)dr\,; \quad A3_{ij} = \int_0^1 \frac{X_i(r)X_j'(r)}{r}\frac{1}{r}\left(\frac{1}{r}\frac{\partial\phi}{\partial r} + \frac{1}{r}\frac{\partial\psi_\infty}{\partial r}\right)dr \tag{67,68}$$

$$B_i = \int_0^1 \frac{X_i(r)}{r}\left(\frac{\partial^4\phi}{\partial r^4} - \frac{2}{r}\frac{\partial^3\phi}{\partial r^3} + \frac{3}{r^2}\frac{\partial^2\phi}{\partial r^2} - \frac{3}{r^3}\frac{\partial\phi}{\partial r} + \frac{d^4\psi_\infty}{dr^4} - \frac{2}{r}\frac{d^3\psi_\infty}{dr^3} + \frac{3}{r^2}\frac{d^2\psi_\infty}{dr^2} - \frac{3}{r^3}\frac{d\psi_\infty}{dr}\right)dr \tag{69}$$

$$C_{ij} = \int_0^1 \Gamma_i(r)X_j(r)\frac{\partial T}{\partial r}dr\,; \quad D_{ij} = \int_0^1 \Gamma_i(r)\Gamma_j(r)\left(\frac{\partial\phi}{\partial r} + \frac{d\psi_\infty}{dr}\right)dr \tag{70,71}$$

$$E_i = \int_0^1 r\Gamma_i(r)\mu\left(\frac{1}{r}\frac{\partial^2\phi}{\partial r^2} - \frac{1}{r^2}\frac{\partial\phi}{\partial r} + \frac{1}{r}\frac{d^2\psi_\infty}{dr^2} - \frac{1}{r^2}\frac{d\psi_\infty}{dr}\right)^2 dr\,; \quad \bar{f}_i = -\frac{1}{2}\frac{1}{M_i}\int_0^1 r(1-r^2)E^2 X_i dr \tag{72,73}$$

$$\bar{g}_i = \frac{1}{N_i}\int_0^1 r\Gamma_i(r)dr \tag{74}$$

In order to handle numerically the ordinary differential equation (ODE) system given by Eqs. (61) to (74) through the subroutine DIVPAG of IMSL Library (1991), it is necessary to truncate the infinite series a sufficiently high number of terms (NV and NT for the velocity and temperature fields, respectively) so as to guarantee the requested relative error in obtaining the original potentials. This subroutine solves initial-value problems with stiff behavior, and provides the important feature of automatically controlling the relative error in the solution of the ODE system, allowing the user to establish error targets for the transformed potentials.

Once the transformed potentials are available, the velocity field is obtained from the definition of the streamfunction given by Eqs. (16) and (17), after introducing the inverse formula (58), to yield

$$v_r(r,z) = \sum_{i=1}^{\infty}\frac{X_i(r)}{r}\frac{d\bar{\phi}_i(z)}{dz}; \quad v_z(r,z) = 2\left(1-r^2\right) - \sum_{i=1}^{\infty}\frac{X_i'(r)}{r}\bar{\phi}_i(z) \tag{75,76}$$

The dimensionless average temperature is defined in the form

$$T_{av}(z) = 2\int_0^1 r v_r(r,z)T(r,z)dr \tag{77}$$

And after introducing the inverse formulas (58) and (60), it results

$$T_{av}(z) = \sum_{i=1}^{\infty} K_i\bar{T}_i(z); \quad K_i = \left[L_i + \sum_{j=1}^{\infty} O_{ij}\bar{\phi}_j(z)\right]; \quad L_i = -2\int_0^1 \Gamma_i(r)\frac{d\psi_\infty}{dr}dr\,; \quad O_{ij} = -2\int_0^1 \Gamma_i(r)X_j'(r)dr \tag{78-81}$$

The local Nusselt number can be calculated from its usual definition as

$$Nu(z) = \frac{h(z^*)2r_w}{k} = -\frac{2}{T_{av}(z)}\frac{\partial T(1,z)}{\partial r} = -\frac{2}{T_{av}(z)}\sum_{i=1}^{\infty}\frac{d\Gamma_i(1)}{dr}\bar{T}_i(z) \tag{82}$$

3. RESULTS AND DISCUSSION

Numerical results for the Nusselt numbers were produced along the entrance region of a circular tube. The computational code was developed in FORTRAN 90/95 programming language. The routine DIVPAG from the IMSL Library (1991) was used to handle numerically the truncated version of the system of ordinary differential equations [Eqs. (61) – (74)], with a relative error target of 10^{-8} prescribed by the user, for the transformed potentials. For the velocity field, the results were produced with different truncation orders (NV ≤ 140) and for Re = 2000, but it should be noted that the dimensionless axial coordinate $X^+ = z/(2Re)$ makes the flow results independent of the Reynolds number for the boundary-layer formulation. Similarly, for the temperature field, the related results were constructed with NV = NT ≤ 140, Re = 2000, Pr = 0.7 and 2 and Br = 0.0, 0.1 and 0.01, along the dimensionless axial coordinate $X^+ = z/(2\,Re)$.

ISSN 2176-5480

The convergence behavior of local Nusselt numbers is analyzed in Tables 1 to 3 for different Prandtl and Brinkman numbers. One verifies excellent convergence rates for all cases analyzed, which is fully reached with four significant digits with N<140 terms in the summations.

Table 1: Convergence behavior of the local Nusselt numbers for Pr = 0.7 and 2.0 and Br = 0.0.

X^*	Pr = 0.7				Pr = 2.0			
	N = 80	N = 100	N = 120	N = 140	N = 80	N = 100	N = 120	N = 140
$1.000\ x10^{-3}$	13.82	13.81	13.79	13.79	11.99	11.98	11.97	11.97
$1.071\ x10^{-3}$	13.37	13.36	13.35	13.34	11.62	11.61	11.60	11.59
$1.429\ x10^{-3}$	11.64	11.63	11.62	11.62	10.20	10.19	10.18	10.18
$1.500\ x10^{-3}$	11.38	11.37	11.36	11.36	9.984	9.974	9.968	9.963
$1.786\ x10^{-3}$	10.49	10.48	10.47	10.47	9.250	9.241	9.236	9.232
$2.000\ x10^{-3}$	9.954	9.946	9.940	9.936	8.811	8.804	8.799	8.795
$2.143\ x10^{-3}$	9.645	9.637	9.631	9.628	8.557	8.550	8.545	8.542
$2.857\ x10^{-3}$	8.483	8.477	8.473	8.469	7.599	7.594	7.591	7.588
$3.000\ x10^{-3}$	8.304	8.298	8.294	8.291	7.452	7.447	7.444	7.441
$3.571\ x10^{-3}$	7.706	7.701	7.698	7.695	6.957	6.953	6.951	6.949
$4.000\ x10^{-3}$	7.348	7.344	7.341	7.339	6.661	6.658	6.655	6.654
$5.000\ x10^{-3}$	6.712	6.708	6.706	6.704	6.133	6.130	6.129	6.127
$6.000\ x10^{-3}$	6.252	6.249	6.246	6.245	5.751	5.749	5.747	5.746
$7.143\ x10^{-3}$	5.857	5.854	5.853	5.851	5.424	5.422	5.421	5.420
$8.000\ x10^{-3}$	5.622	5.602	5.619	5.618	5.229	5.228	5.227	5.227
$1.000\ x10^{-2}$	5.208	5.206	5.205	5.204	4.888	4.887	4.886	4.886
$1.071\ x10^{-2}$	5.092	5.091	5.089	5.089	4.793	4.792	4.791	4.791
$1.429\ x10^{-2}$	4.663	4.662	4.661	4.661	4.442	4.441	4.441	4.441
$1.500\ x10^{-2}$	4.599	4.599	4.598	4.597	4.390	4.389	4.389	4.389
$1.786\ x10^{-2}$	4.391	4.391	4.390	4.389	4.220	4.219	4.219	4.219
$2.000\ x10^{-2}$	4.273	4.272	4.272	4.271	4.124	4.123	4.123	4.123
$2.143\ x10^{-2}$	4.206	4.206	4.205	4.205	4.069	4.069	4.069	4.069
$2.857\ x10^{-2}$	3.979	3.978	3.978	3.978	3.886	3.886	3.886	3.886
$3.571\ x10^{-2}$	3.853	3.852	3.852	3.852	3.787	3.787	3.787	3.787
$7.143\ x10^{-2}$	3.679	3.679	3.679	3.679	3.665	3.665	3.665	3.665
$7.661\ x10^{-2}$	3.673	3.673	3.673	3.673	3.663	3.662	3.663	3.663
$1.071\ x10^{-1}$	3.660	3.660	3.660	3.660	3.657	3.657	3.657	3.657
$2.000\ x10^{-1}$	3.657	3.657	3.657	3.657	3.657	3.657	3.657	3.657
1.000	3.657	6.657	3.657	3.657	3.657	3.657	3.657	3.657

N = NV = NT.

Table 2: Convergence behavior of the local Nusselt numbers for Pr = 0.7 and 2.0 and Br = 0.1.

X^*	Pr = 0.7				Pr = 2.0			
	N = 80	N = 100	N = 120	N = 140	N = 80	N = 100	N = 120	N = 140
$1.000\ x10^{-3}$	13.75	13.74	13.73	14.73	11.95	11.94	11.93	11.93
$1.071\ x10^{-3}$	13.30	13.29	13.28	13.27	11.58	11.57	11.56	11.56
$1.429\ x10^{-3}$	11.57	11.56	11.55	11.55	10.16	10.15	10.14	10.14
$1.500\ x10^{-3}$	11.30	11.29	11.29	11.28	9.946	9.936	9.929	9.925
$1.786\ x10^{-3}$	10.41	10.40	10.39	10.39	9.213	9.205	9.199	9.196
$2.000\ x10^{-3}$	9.878	9.870	9.865	9.861	8.776	8.768	8.763	8.760
$2.143\ x10^{-3}$	9.569	9.561	9.557	9.553	8.522	8.515	8.511	8.508
$2.857\ x10^{-3}$	8.409	8.403	8.399	8.396	7.568	7.563	7.559	7.557
$3.000\ x10^{-3}$	8.230	8.225	8.221	8.218	7.421	7.416	7.413	7.411
$3.571\ x10^{-3}$	7.634	7.629	7.626	7.624	6.929	6.925	6.922	6.921
$4.000\ x10^{-3}$	7.279	7.274	7.271	7.269	6.634	6.631	6.628	6.627

ISSN 2176-5480

Table 2: Continued.

X^*	Pr = 0.7				Pr = 2.0			
	N = 80	N = 100	N = 120	N = 140	N = 80	N = 100	N = 120	N = 140
5.000×10^{-3}	6.646	6.642	6.639	6.638	6.109	6.106	6.105	6.103
6.000×10^{-3}	6.189	6.186	6.184	6.182	5.729	5.727	5.726	5.725
7.143×10^{-3}	5.798	5.795	5.794	5.792	5.404	5.403	5.402	5.401
8.000×10^{-3}	5.566	5.564	5.562	5.561	5.212	5.211	5.209	5.209
1.000×10^{-2}	5.157	5.155	5.154	5.153	4.874	4.872	4.871	4.871
1.071×10^{-2}	5.043	5.041	5.040	5.039	4.779	4.778	4.778	4.777
1.429×10^{-2}	4.621	4.620	4.619	4.619	4.432	4.431	4.431	4.430
1.500×10^{-2}	4.559	4.558	4.557	4.557	4.381	4.379	4.379	4.379
1.786×10^{-2}	4.355	4.354	4.354	4.353	4.212	4.212	4.212	4.211
2.000×10^{-2}	4.239	4.239	4.238	4.238	4.117	4.117	4.116	4.116
2.143×10^{-2}	4.175	4.174	4.174	4.174	4.064	4.063	4.063	4.063
2.857×10^{-2}	3.955	3.954	3.954	3.954	3.883	3.882	3.882	3.882
3.571×10^{-2}	3.834	3.834	3.834	3.834	3.785	3.785	3.785	3.785
7.143×10^{-2}	3.673	3.673	3.673	3.673	3.665	3.665	3.665	3.665
7.661×10^{-2}	3.668	3.668	3.668	3.668	3.662	3.662	3.662	3.662
1.071×10^{-1}	3.658	3.658	3.658	3.658	3.657	3.657	3.657	3.657
2.000×10^{-1}	3.657	3.657	3.657	3.657	3.657	3.657	3.657	3.657
1.000	3.657	3.657	3.657	3.657	3.657	3.657	3.657	3.657

N = NV = NT.

Table 3: Convergence behavior of the local Nusselt numbers for Pr = 0.7 and 2.0 and Br = 0.01.

X^*	Pr = 0.7				Pr = 2.0			
	N = 80	N = 100	N = 120	N = 140	N = 80	N = 100	N = 120	N = 140
1.000×10^{-3}	13.81	13.80	13.79	13.78	11.99	11.98	11.97	11.96
1.071×10^{-3}	13.37	13.35	13.34	13.33	11.63	11.61	11.59	11.58
1.429×10^{-3}	11.63	11.62	11.62	11.61	10.21	10.19	10.18	10.17
1.500×10^{-3}	11.37	11.36	11.35	11.35	9.975	9.970	9.964	9.963
1.786×10^{-3}	10.49	10.47	10.46	10.46	9.245	9.238	9.232	9.230
2.000×10^{-3}	9.943	9.938	9.932	9.929	8.806	8.800	8.795	8.792
2.143×10^{-3}	9.632	9.629	9.624	9.921	8.549	8.547	8.542	8.538
2.857×10^{-3}	8.470	8.469	8.465	8.462	7.595	7.591	7.588	7.585
3.000×10^{-3}	8.295	8.291	8.287	8.284	7.447	7.444	7.441	7.437
3.571×10^{-3}	7.698	7.694	7.691	7.688	6.953	6.951	6.948	6.945
4.000×10^{-3}	7.339	7.337	7.334	7.332	6.658	6.655	6.652	6.650
5.000×10^{-3}	6.707	6.702	6.699	6.697	6.131	6.128	6.126	6.124
6.000×10^{-3}	6.244	6.242	6.240	6.239	5.749	5.747	5.745	5.743
7.143×10^{-3}	5.850	5.848	5.847	5.846	5.423	5.420	5.419	5.417
8.000×10^{-3}	5.618	5.615	5.613	5.612	5.229	5.227	5.226	5.225
1.000×10^{-2}	5.205	5.201	5.199	5.199	4.888	4.886	4.885	4.884
1.071×10^{-2}	5.087	5.086	5.085	5.084	4.794	4.791	4.790	4.789
1.429×10^{-2}	4.660	4.658	4.657	4.657	4.443	4.440	4.440	4.439
1.500×10^{-2}	4.596	4.595	4.594	4.594	4.391	4.389	4.388	4.388
1.786×10^{-2}	4.388	4.387	4.387	4.386	4.220	4.219	4.219	4.218
2.000×10^{-2}	4.269	4.269	4.268	4.268	4.124	4.123	4.122	4.121
2.143×10^{-2}	4.204	4.203	4.202	4202	4.070	4.069	4.069	4.067
2.857×10^{-2}	3.977	3.976	3.976	3.976	3.887	3.886	3.886	3.885
3.571×10^{-2}	3.853	3.851	3.851	3.850	3.788	3.787	3.787	3.786
7.143×10^{-2}	3.679	3.678	3.678	3.678	3.665	3.665	3.665	3.665
7.661×10^{-2}	3.673	3.672	3.672	3.672	3.663	3.663	3.662	3.662
1.071×10^{-1}	3.661	3.660	3.659	3.659	3.657	3.657	3.657	3.657
2.000×10^{-1}	3.657	3.657	3.657	3.657	3.657	3.657	3.657	3.657
1.000	3.657	3.657	3.657	3.657	3.657	3.657	3.657	3.657

N = NV = NT.

ISSN 2176-5480

In order to demonstrate the consistency of the final results, Table 4 shows a set of benchmark results for the local Nusselt numbers along the tube length for Pr = 0.7 and 2.0 and Br = 0.0. It is possible to realize that the results have a good agreement when compared with the numerical results presented in the literature. At some positions near the entrance, a more marked difference among the sets of results is verified between the present work and those of Paz et al. (2007), which have employed the same solution methodology. This difference can be explained due to the present work have used semi-analytical integration to calculate the integral coefficients and Paz et al. (2007) have used analytical integrations that certainly affected the final results.

Table 4: Reference results for the local Nusselt numbers for Pr = 0.7 and 2.0 and Br = 0.0.

X^*	Pr = 0.7			Pr = 2.0		
	Present	Paz et al. (2007)	Shah and London	Present	Paz et al. (2007)	Shah and London
1.000 x10^{-3}	13.79	12.83	12.6 [a]	11.97	11.61	11.4 [a]
1.071 x10^{-3}	13.34	12.45	12.4 [b] /11.94 [c]	11.59	11.28	-
1.429 x10^{-3}	11.62	11.00	11.0 [b] /10.65 [c]	10.18	10.00	-
1.500 x10^{-3}	11.36	10.77	10.8 [a]	9.963	9.807	9.8 [a]
1.786 x10^{-3}	10.47	10.01	9.99 [b] /9.757 [c]	9.232	9.137	-
2.000 x10^{-3}	9.936	9.546	9.6 [a]	8.795	8.733	8.8 [a]
2.143 x10^{-3}	9.628	9.277	9.26 [b] /9.086 [c]	8.542	8.497	-
2.857 x10^{-3}	8.469	8.253	8.24 [b] /8.129 [c]	7.588	7.598	-
3.000 x10^{-3}	8.291	8.094	8.2 [a]	7.441	7.457	7.5 [a]
3.571 x10^{-3}	7.695	7.556	7.54 [b] /7.469 [c]	6.949	6.985	-
4.000 x10^{-3}	7.339	7.232	7.3 [a]	6.654	6.699	6.8 [a]
5.000 x10^{-3}	6.704	6.647	6.7 [a]	6.127	6.184	6.2 [a]
6.000 x10^{-3}	6.245	6.218	6.25 [a]	5.746	5.806	5.8 [a]
7.143 x10^{-3}	5.851	5.846	5.84 [b] /5.793 [c]	5.420	5.479	-
8.000 x10^{-3}	5.618	5.624	5.60 [a]	5.227	5.284	5.3 [a]
1.000 x10^{-2}	5.204	5.226	5.25 [a]	4.886	4.935	4.93 [a]
1.071 x10^{-2}	5.089	5.114	5.11 [b] /5.081 [c]	4.791	4.837	-
1.429 x10^{-2}	4.661	4.695	4.69 [b] /4.671 [c]	4.441	4.474	-
1.500 x10^{-2}	4.597	4.632	4.60 [a]	4.389	4.420	4.44 [a]
1.786 x10^{-2}	4.389	4.425	4.42 [b] /4.409 [c]	4.219	4.243	-
2.000 x10^{-2}	4.271	4.305	4.28 [a]	4.123	4.142	4.17 [a]
2.143 x10^{-2}	4.205	4.238	4.23 [b] /4.224 [c]	4.069	4.086	-
2.857 x10^{-2}	3.978	4.002	3.998 [b] /3.993 [c]	3.886	3.896	-
3.571 x10^{-2}	3.852	3.869	3.846 [b] /3.862 [c]	3.787	3.793	-
7.143 x10^{-2}	3.679	3.681	3.641 [b] /3.674 [c]	3.665	3.666	-
7.661 x10^{-2}	3.673	3.675	3.632 [b]	3.663	3.663	-
1.071 x10^{-1}	3.660	3.660	3.655 [c]	3.657	3.657	-
2.000 x10^{-1}	3.657	3.657	3.66 [a]	3.657	3.657	3.66 [a]
1.000	3.657	3.657	3.66 [a]	3.657	3.567	3.66 [a]

[a]Graphical results of Honbeck (Hornbeck, 1965); [b]Manohar (Shah and London, 1978);
[c]Hwang (Shah and London, 1978).

4. CONCLUSIONS

The GITT was successfully employed in the solution of the boundary layer equations in the simultaneously developing flow of Newtonian fluids in circular tubes to study the effect of viscous dissipation in the temperature field. The streamfunction formulation was preferred aimed at dealing with the singularity at the channel centerline. Benchmark results for the local Nusselt numbers in the entrance region were then tabulated for different Prandtl and Brinkman numbers. The numerical results obtained showed that the local Nusselt number is a monotonically decreasing function of the dimensionless axial coordinate and that tends to be uniform independently of the Prandtl or Brinkman number. The good agreement of the present results with previously reported ones demonstrates the consistency of this approach and adequacy for benchmarking this class of problems.

5. REFERENCES

Campos Silva, J. B., Cotta, R.M. and Aparecido, J. B., 1992. *Analytical solutions to simultaneously developing laminar flow inside parallel-plates channel.* International Journal of Heat and Mass Transfer;35:887–895.

Cotta, R. M., 1990. *Hybrid numerical–analytical approach to nonlinear diffusion problems.* Numerical Heat Transfer,Part B—Fundamentals; 17:217–226.

Cotta, R. M., 1993. *Integral Transforms in Computational Heat and Fluid Flow*, CRC Press, Boca Raton, USA.

Cotta, R. M., 1998. *The Integral Transform Method in Thermal and Fluid Sciences and Engineering.* Begell House: New York, U.S.A.

Cotta, R. M., Santos, C. A. C., Quaresma, J. N. N. and Perez-Guerrero, J. S., 2005. *Hybrid integral transforms in convection-diffusion: recent applications in internal flow simulation, invited lecture.* Proceedings of the 4th International Conference on Computational Heat and Mass Transfer, 4th ICCHMT, vol. 1, Paris-Cachan, France; 153–164.

Cotta, R. M. and Mikhailov, M. D., 2006. *Hybrid methods and symbolic computations.* In Handbook of Numerical Heat Transfer (2nd edn), Chapter 16, Minkowycz WJ, Sparrow EM, Murthy JY (eds). Wiley: New York, U.S.A.; 493–522.

Dehkordi, A. M. and Memari, M., 2010. *Transient and steady-state forced convection to power-law fluids in the thermal entrance region of circular ducts: Effects of viscous dissipation, variable viscosity, and axial conduction.* Energy Conversion and Management, vol. 51, pp. 1065–1074.

Dehkordi, A. M. and Mohammadi, A. A., 2009. *Transient forced convection with viscous dissipation to power-law fluids in thermal entrance region of circular ducts with constant wall heat flux.* Energy Conversion and Management, vol. 50, pp. 1062–1068.

IMSL Library, 1991. MATH/LIB, Houston, TX.

Machado, H. A. and Cotta, R.M., 1995. *Integral transform method for boundary layer equations in simultaneous heat and fluid flow problems.* International Journal of Numerical Methods for Heat and Fluid Flow;5:225–237.

Paz, S. P. A., Macêdo, E. N., Quaresma, J. N. N. and Cotta, R. M., 2007. *Eigenfunction expansion solution for boundary-layer equations in cylindrical coordinates: simultaneously developing flow in circular tubes.* Numerical Heat Transfer, Part A—Applications;52:1123–1149.

Pereira, L. M., Perez-Guerrero, J. S. and Cotta, R. M., 2000. *Analysis of laminar forced convection in annular ducts using integral transforms.* Hybrid Methods in Engineering;2:221–232.

Perez-Guerrero, J. S. and Cotta, R. M., 1992. *Integral transform method for Navier–Stokes equations in stream function-only formulation.* International Journal for Numerical Methods in Fluids;15:399–409.

Perez-Guerrero, J. S., Quaresma, J. N. N. and Cotta, R. M., 2000. *Simulation of laminar flow inside ducts of irregular geometry using integral transforms.* Computational Mechanics;25:413–420.

Santos, C. A. C., Quaresma, J. N. N. and Lima, J. A., 2001. *Benchmark Results for Convective Heat Transfer in Ducts: The Integral Transform Approach.* ABCM Mechanical Sciences Series. Editora E-Papers: Rio de Janeiro, Brazil.

Shah, R. K. and London, A. L., *Laminar Flow Forced Convection in Ducts, Advances in Heat Transfer*, Supplement 1, Academic Press, New York, 1978.

Hornbeck, R. W., *An All-Numerical Method for Heat Transfer in the Inlet of a Tube*, Proc. ASME, Winter Annual Meeting, Chicago, 1965, Paper 65-WA=HT-36.